

Hybrid Polymer-Grafted Multiwalled Carbon Nanotubes for In vitro Gene Delivery

Antonio Nunes, Nadja Amsharov, Chang Guo, Jeroen Van den Bossche, Padmanabhan Santhosh, Theodoros K. Karachalios, Stephanos F. Nitodas, Marko Burghard, Kostas Kostarelos,* and Khuloud T. Al-Jamal*

Carbon nanotubes (CNTs) consist of carbon atoms arranged in sheets of graphene rolled up into cylindrical shapes. This class of nanomaterials has attracted attention because of their extraordinary properties, such as high electrical and thermal conductivity. In addition, development in CNT functionalization chemistry has led to an enhanced dispersibility in aqueous physiological media which indeed broadens the spectrum for their potential biological applications including gene delivery. The aim of this study is to determine the capability of different cationic polymer-grafted multiwalled carbon nanotubes (MWNTs) (polymer-g-MWNTs) to efficiently complex and transfer plasmid DNA (pCMV- β Gal) in vitro without promoting cytotoxicity. Carboxylated MWNT is chemically conjugated to the cationic polymers polyethylenimine (PEI), polyallylamine (PAA), or a mixture of the two polymers. In order to explore the potential of these polymer-g-MWNTs as gene delivery systems, we first study their capacity to complex plasmid DNA (pDNA) using agarose gel electrophoresis. Gel migration studies confirm pDNA binding to polymer-g-MWNT with different affinities, highest for PEI-g-MWNT and PEI/PAA-g-CNT constructs. β -galactosidase expression is assessed in human lung epithelial (A549) cells, and the cytotoxicity is determined by modified LDH assay after 24 h incubation period. Additionally, PEI-g-MWNT and/or PEI/PAA-g-MWNT reveal an improvement in gene expression when compared to the naked pDNA or to the equivalent amounts of PEI polymer alone. Mechanistically, pDNA was delivered by the polymer-g-MWNT constructs via a different pathway compared to those used by polyplexes. In conclusion, polymer-g-MWNTs may be considered in the future as a versatile tool for efficient gene transfer in cancer cells in vitro, provided their toxicological profile is established.

A. Nunes, Dr. C. Guo, Dr. J. V. den Bossche, Prof. K. Kostarelos,
Dr. K. T. Al-Jamal
Nanomedicine Laboratory
Centre for Drug Delivery Research, The School of Pharmacy
University of London, WC1N 1AX, UK
E-mail: kostas.kostarelos@pharmacy.ac.uk; khuloud.al-jamal@
pharmacy.ac.uk

Dr. N. Amsharov, Dr. P. Santhosh, Dr. M. Burghard
Nanoscale Science Department
Max-Planck-Institute for Solid State Research
Heisenbergstrasse 1, 70569 Stuttgart, Germany
Dr. P. Santhosh
Department of Nanoengineering
University of California San Diego
La Jolla, California 92093-0448, USA
T. K. Karachalios, Dr. S. F. Nitodas
Nanothinx S.A., Stadiou Str.
Rio-Patras, 26504, Greece

DOI: 10.1002/sml.201000864

1. Introduction

Gene therapy is an emerging field that aims to correct genetic disorders at the molecular level. The main requirement for its success is the generation of a vector that protects exogenous DNA from degradation and achieves effective cell translocation. In addition, the resulting DNA-vector complex should result in subsequent intracellular release with low toxicity levels.^[1] Hence, an effective delivery system is vital to achieve successful gene delivery.^[1,2] For this purpose viral (e.g., adenovirus, and retrovirus) and nonviral (polymers,^[1,4,5] nanoparticles,^[1,4,6] and liposomes^[7]) vectors have been developed. Viral vectors are the most effective gene transfer vectors, but suffer from immunogenic responses. Nonviral vectors exhibit a much better immunogenic profile, however still lacking the efficiency of the viral vectors.

Recently, a novel type of nonviral gene vector has emerged, based on functionalized carbon nanotubes (*f*-CNT). Various types of nanotube chemical functionalization approaches have led to improvements in their dispersibility in physiological media that broaden the spectrum of potential biological applications.^[2,3,8,9] *f*-CNT possess unique features that make them extremely attractive for the construction of novel gene delivery vectors. Most importantly, they have the ability to interact with biological components and be internalized efficiently in different cell types by different mechanisms.^[10,12] Several studies have shown promising results, exploiting *f*-CNT characteristics for plasmid DNA (pDNA) and short interfering RNA (siRNA) delivery in vitro and in vivo.^[2,3,12,17]

Three types of *f*-CNT have been described for pDNA delivery. The first type was reported by our group and includes CNT chemically modified with aminated tetraethylene glycol functionalities to demonstrate the feasibility of *f*-CNT as carriers for gene delivery.^[2] We reported that pDNA was able to associate in a condensed globular conformation through electrostatic interactions onto the surface of *f*-CNT at specific charge ratios. The results showed 500 times higher levels of gene expression compared to naked pDNA and the lack of cytotoxicity of the complex was also demonstrated.^[2] In another study, we reported the gene transfer efficiency between different types of CNT chemically functionalized with alternative cationic head groups (i.e., single-walled carbon nanotube- (SWNT)-NH₃⁺, multiwalled carbon nanotube- (MWNT)-NH₃⁺, and SWNT-Lys-NH₃⁺). We concluded that the surface area (length and width) and charge density of the *f*-CNT were the critical parameters for the interaction with pDNA and the consequent formation of a biologically active complex.^[3] Along similar lines, Gao et al.^[12] have also investigated the ability of *f*-CNT modified with amino-, carboxyl-, hydroxyl-, and alkyl-functions for pDNA delivery in vitro and concluded that the positively charged amino-*f*-MWNT was effective in pDNA complexation and delivery. However, the efficiency of these *f*-CNT did not reach transfection levels as these of commercially available reagents.^[12] The second class of *f*-CNT used for pDNA delivery includes CNT functionalized with polymers such as polyethyleneimine (PEI). Liu et al.^[15] published the first study using PEI-grafted-CNT as a pDNA carrier, showing

the ability of MWNT grafted with branched PEI (25 kDa) to immobilize pDNA onto the nanotube surface and the capability of these complexes to enhance gene expression.^[15] More recently, SWNTs were chemically functionalized with cationic glycopolymers to achieve gene transfer in vitro.^[18] Glycopolymer-*g*-SWNT were complexed with plasmid enhanced green fluorescent protein (EGFP) and both transfection efficiency and cell viability were shown to be similar to Lipofectamine 2000.^[18] Finally, a third approach included physical adsorption of cationic phospholipids or polymers on the CNT surface able to complex pDNA. For this approach, chitosan (NG042) was adsorbed on the surface of SWNT and used for the delivery of pDNA encoding the eGFP reporter. Even though no gene expression studies were described in that work, it was shown that SWNT:NG042 increased the intracellular delivery of pDNA.^[19]

The aim of the present study was to evaluate the capability of a combination of polymers grafted by peptide coupling chemistry onto MWNT to generate different types of polymer-grafted-MWNT (polymer-*g*-MWNT) able to condense pDNA efficiently and enhance gene expression in vitro. For this purpose we selected two polymers; PEI which is a widely used transfection reagent due to its high amine content and the capacity to escape the endosomal compartments through the proton sponge effect.^[4,20] These features lead to pDNA complexation, disruption of endosomal membrane and subsequent release of the PEI:pDNA complexes intracellularly.^[4,20] However, PEI suffers from an unfavorable cytotoxicity profile. The second polymer selected was polyallylamine (PAA), a linear cationic polymer that has attracted attention for its potential as a nonviral gene delivery carrier^[1,21] due to its high density of primary amine groups and consequently, the strong positive charge at physiological pH.^[1] However, the large number of available primary amino groups can also lead to high cytotoxicity. Therefore, PAA requires chemical modification using specific ligands capable of receptor-mediated endocytosis or added lysosomotropic agents to achieve efficient gene delivery.^[1,22] Thus we hypothesized that MWNT functionalized with PEI-PAA hybrids (PEI/PAA-*g*-MWNT) could offer improved gene transfer in vitro compared to MWNT functionalized with the individual polymers (PEI-*g*-MWNT or PAA-*g*-MWNT). Such enhancements in gene transfer vector technology could be beneficial as reduced vector concentrations may be required to achieve adequate levels of gene expression, in that way eliminate the cytotoxicity induced by cationic, polymer-based nonviral gene vectors.

2. Experimental

2.1. Materials

MWNTs were provided by Nanothinx (Rio Patras, Greece; Batch # NTX99%_122007). Outer average diameter was 200 nm, and length ranged between 0.5–2 μm. All chemicals and solvents were used as received. Milli-Q water was used in all experiments. Polyethyleneimine (25 000 Da), polyallylamine (60 000 Da), *N*-ethyl-*N'*-(3-dimethylaminopropyl)

carbodiimide hydrochloride, Tris/borate/ethylenediamine-tetraacetic acid (EDTA) buffer (TBE buffer), and ethidium bromide were obtained from Sigma-Aldrich (USA). The orange loading dye solution was purchased from Fermentas (UK).

Human lung carcinoma (A549) cell line was purchased from American Type Culture Collection (ATCC) (USA) (ATCC# CCL-185) cultured in Dulbecco's Modified Eagle Medium (DMEM) or Kaighn's modification of Ham's F-12 nutrient medium (F-12). Cell culture medium, fetal bovine serum (FBS), penicillin/streptomycin, phosphate buffered saline (PBS), electrophoresis grade Agarose, and TO-PRO-3 nuclear counterstaining dye were purchased from Gibco, Invitrogen (UK). The 400-mesh copper grids coated with formvar/carbon support film used for TEM were from Agar Scientific (UK). Gigapreps of highly purified supercolloid plasmid DNA of the reported gene pCMV- β -Galactosidase (BD-Clontech, UK) were prepared by Bayou Biolabs (USA). Stock solution of 10 mg mL⁻¹ in deionised water were diluted in aliquots of 1 mg mL⁻¹ and stored in at -20 °C until needed. For β -Gal assay, Tropix Galacto-light Plus kit from Applied Biosystem (UK) was used. The kit includes lysis solution, substrate buffer and accelerator II. The white-96-well plates used for the assay were purchased from Greiner (UK). LDH release was assessed using Promega Cytotox 96 non-radioactive cytotoxicity assay (Promega UK Ltd). Anti-EEA1 was purchased from Transduction Laboratories (USA) and Cy3-conjugated goat anti-mouse was used as secondary antibodies (Jackson ImmunoResearch, West Grove, PA). Fluorescein labeled pDNA was obtained from Cambridge Bioscience (UK) and used for uptake studies. Vectashield mounting medium was obtained from Vector Laboratories (CA, USA).

2.2. Chemical Functionalization of Multiwalled Carbon Nanotubes (f-MWNT)

Pristine MWNT was first oxidized (carboxylated) by treating the material sample with nitric acid (HNO₃). The sample was subsequently ultrasonicated for 10 min in HNO₃ 65% (100 mL per 1 g of CNTs in powder form); the solution was mechanically stirred at 220 °C for 20 min, cooled down to room temperature, filtered and finally dried at room temperature.^[23] Polymer-g-MWNTs were prepared by conjugation of the activated carboxylic acid groups of oxidized carbon nanotubes to the amino groups of the cationic polymers (PEI, PAA, or a combination of PEI and PAA) by peptide coupling chemistry using *N*-ethyl-*N*-(3-dimethylaminopropyl)-carbodiimide hydrochloride (EDCI) as a coupling reagent as shown in **Scheme 1**. For the preparation of PEI-g-MWNT, the PEI (1 mg mL⁻¹) was reacted with a suspension of oxidized MWNT (3 mg mL⁻¹, pH 6.2). For the preparation of PAA-g-MWNT, the PAA (2.5 mg mL⁻¹) was reacted with a suspension of oxidized MWNT (1 mg mL⁻¹, pH 4.5). For the

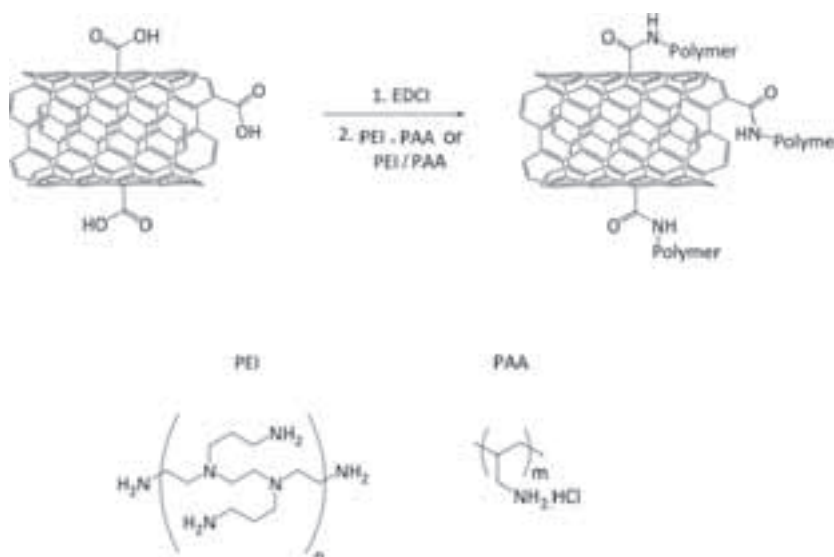
preparation of PEI/PAA-g-MWNT, PEI (3 mg mL⁻¹) and PAA (25 mg mL⁻¹) were both reacted with a suspension of oxidized MWNT (3 mg mL⁻¹, pH 6.2). The optimum concentration of PEI and PAA used for grafting was optimised based on the dispersibility and the stability of the resultant polymer-g-MWNT conjugates. EDCI was used in all reactions as a coupling reagent at 150 mg mL⁻¹ concentration. The pH of each of MWNT dispersion had been previously adjusted to the required value with HCl, before polymer addition. The mixture obtained was sonicated for 1 h and stirred for 10 h at room temperature (RT). After centrifugation at 13 000 rpm for 30 min, the supernatant was discarded. The washing procedure was repeated thrice for complete removal of unreacted polymer. Finally the corresponding polymer-g-MWNT was collected and dried under vacuum.

2.3. Transmission Electron Microscopy (TEM) and Scanning Electron Microscopy (SEM)

Pristine MWNT, oxidized MWNT (MWNT-COOH), and polymer-g-MWNT powders were hydrated in 5% dextrose at 1 mg mL⁻¹ concentration by bath-sonication for 15 min (VWR ultrasonic cleaner, UK). The sonicated MWNT dispersions were deposited on 400-mesh copper grids coated with formvar/carbon support film and allowed to dry at RT before imaging under a transmission electron microscope (Philips CM10). The acceleration voltage used was 80 KV. The images were captured with a high-resolution digital camera coupled to the TEM microscope. SEM (Ultra 55, Gemini, ZEISS, Germany) was also used for the characterization of the polymer-g-MWNT (data not shown).

2.4. NMR Spectroscopy

A stock solution of 10 mg mL⁻¹ of PEI was dissolved in D₂O, and of this stock 0.07, 0.125, 0.25, 0.5, and 1 mg



Scheme 1. Synthesis of the polymer-g-MWNTs used in vitro.

PEI samples were measured using a syringe. MWNT-COOH (250 μg) was added to each sample and the mixture was sonicated until a stable dispersion was obtained. Finally, 1 mg t-BuOH was added to each sample as an internal standard in CDCl_3 . For NMR analysis of the PEI-g-MWNT samples, 250 and 500 μg , were sonicated in 0.5 mL D_2O until a stable suspension was obtained and 1 mg t-BuOH was added to these samples. NMR spectra of these samples were acquired using a Bruker 400 MHz spectrometer and the ratio of the integrals of the PEI peaks versus the integral of t-BuOH was plotted versus the amount of PEI. The resulting standard curve was used to calculate the amount of PEI grafted to PEI-g-MWNT.

2.5. Raman Spectroscopy

Raman spectra were collected using a single grating spectrometer (Jobin Yvon Typ labram V 010), equipped with a double super razor edge filter and a peltier cooled charge coupled device (CCD) camera. Spectra were taken in quasi-backscattering geometry using the linearly polarized 632.817 nm line of a He/Ne gas laser with power less than 1 mW, focused to a 5 μm spot through a 100x microscope objective on to the top surface of the sample. The resolution of the spectrometer (grating 1800 L mm^{-1}) was 1 wavenumber (cm^{-1}). For sample preparation, 1 mg of sample (pristine MWNT or polymer-g-MWNT) was suspended in the 1 mL of water. 10 μL of the suspension was dropped on the cleaned Si wafer and dried in the air.

2.6. Agarose Gel Electrophoresis

pDNA complexes were prepared by mixing 0.5 μg of pDNA (pCMV- βGal) (30 μL) with free polymer or polymer-g-MWNT (30 μL) to obtain different polymer:pDNA or polymer-g-MWNT: pDNA mass ratios. Complexes were incubated for 30 min at RT to allow complete complexation to occur. Naked pDNA or the complexes were mixed with orange dye solution (1:10 dilution) and loaded onto 1% (w/v) agarose/TBE gel containing ethidium bromide (EtBr, 0.5 $\mu\text{g mL}^{-1}$). The gel was run for 150 min at 120 mV using electrophoresis unit (BioRad, UK) and 0.5x TBE as a running buffer. Visual tracking of the loading solution monitored the migration of pDNA during electrophoresis. The bands of pDNA were visualized by ethidium bromide staining and imaged by UV light using bioimaging system gene genius (Syngene, UK).

2.7. Gene Expression

A549 cells were maintained in DMEM or Ham's F12 media supplemented with 10% fetal bovine serum (FBS), 50 U mL^{-1} penicillin, 50 $\mu\text{g mL}^{-1}$ streptomycin, 1% L-glutamine, and 1% nonessential amino acids at 37 $^\circ\text{C}$ in 5% CO_2 . Cells were passaged when they reached 80% confluence in order to maintain exponential growth. Cells

were seeded at 25×10^3 cells per well in 24-well plates for 24 h. Before transfection, the complete growth medium was replaced by prewarmed serum-free medium (400 μL), to which 100 μL of polymer-g-MWNT:pDNA or polymer:pDNA complexes containing 1 μg pDNA were added. The complexes were allowed to interact with the cultured cells for 4 h at 37 $^\circ\text{C}$ in humidified atmosphere (5% CO_2). Untreated cells or cells treated just with pDNA (naked group) were used as negative controls. This was replaced with complete media after 4 h. Gene expression was assessed 24 h after incubation; cells were lysed by adding lysis solution (200 μL per well) for 10 min at RT. Cell lysates were centrifuged at 13 000 rpm for 5 min at RT. The analysis of β -gal expression was performed using Tropix Galacto-light Plus TM kit, according to the manufacturer's instructions. Briefly, 10 μL of supernatant was reacted with the reaction buffer (70 μL) in white 96-well plates. The reaction buffer was prepared by diluting Galacton-plus substrate with reaction buffer diluents at 1:100 (v/v) ratio. After incubation for 45 min at RT, the plate was analyzed with a plate reader (FLUOstar Omega, BMG Labtech, UK) using 5 s for measurement and 0.5 s delay between measurements. The relative light unit (RLU) readings were recorded and plotted as RLU per well \pm standard deviation (SD, $n = 3$).

2.8. Intracellular Trafficking of pDNA Complexes in A549 Cells

A549 cells were seeded at density of 25×10^3 cells per coverslip in 24-well plates for 24 h. Before transfection, the complete growth media was washed and replaced by pre-warmed serum-free media (400 μL), to which 100 μL of polymer-g-MWNT:pDNA complexes (at a dose of 1 μg pDNA per well and 10:1 polymer-g-pDNA mass ratio) or polymer:pDNA complexes (at a dose of 1 μg pDNA per well and 1:1 polymer:pDNA mass ratio) was added. The complexes were allowed to interact with the cultured cells for 4 h at 37 $^\circ\text{C}$ in humidified atmosphere (5% CO_2) and replaced with complete media after 4 h. Cells were fixed in 4% paraformaldehyde in PBS for 10 min at RT after treatment for 4 h or 24 h, then rinsed with PBS. For nuclear staining, cells were permeabilized with 0.1% Triton X-100 in PBS for 10 min at 4 $^\circ\text{C}$, RNase treated (100 $\mu\text{g mL}^{-1}$) for 20 min at 37 $^\circ\text{C}$, and incubated with TO-PRO-3 (1 μM) in PBS for 15 min, then rinsed three times with PBS. Nonspecific binding was blocked using PBS containing 4% normal goat serum and 3% bovine serum albumin (blocking buffer). Antibodies were diluted to their final concentration in blocking buffer. Anti-EEA1 antibodies were applied for 2 h at RT. Cells were rinsed once in blocking buffer and three times for 5 min with PBS, and then the secondary antibody was applied for 2 h at RT. Finally, cells were washed five times for 5 min with PBS and mounted onto slides with Vectashield mounting medium. The uptake of fluorescein labeled pDNA was imaged by confocal laser scanning microscopy (CLSM) (Zeiss Axiovert LSM510) using 63x oil immersion objective lens (Carl Zeiss Inc., Thornwood, NY). Fluorescein, Cy3-, and TO-PRO-3 were excited at 488, 543, and 647 nm, respectively. Separate excitation and collection was used to minimize bleed-through.

2.9. Cell Viability

A549 cells were seeded at a density of 25×10^3 cells per well in 24-well plates for 24 h in complete media. Cells were then incubated with the test material for 4 h in serum-free media at 37 °C in humidified atmosphere (5% CO₂). After incubation, media was removed and replaced with fresh complete media for an additional 20 h. Cells were assessed by a modiPac LDH assay.^[24] Media was removed and cells were lysed for 1 h with 9% (v/v) TritonX100 in water (10 μL) mixed with 100 μL phenol-free media (serum-free RPMI media) at RT. Cell lysate was centrifuged at 1600 rpm for 5 min at RT and the supernatant was collected (50 μL) and reacted with LDH reconstituted substrate mixture (50 μL) for 15 min. The reaction was then stopped by DMSO (50 μL) and absorbance was measured at 492 nm in a plate reader (FLUOstar Omega, BMG Labtech, UK). Untreated cells were used as a negative control (100% LDH in healthy cells) and 10% DMSO was used as a positive toxic control. Cell viability was expressed as a percentage of healthy untreated cells (n = 4).

3. Results

Synthesis and characterization of polymer-*g*-MWNT. Three different types of polymer-*g*-MWNT were synthesized for the purpose of this study. First, untreated pristine MWNT were oxidized and then different cationic polymers were grafted onto the carboxylic acid groups of the MWNT as described in Scheme 1. The cationic polymers PEI, PAA, or a PEI/PAA mixture were used to produce PEI-*g*-MWNT, PAA-*g*-MWNT, or PEI/PAA-*g*-MWNT, respectively. The characteristics of the polymer-*g*-MWNT before and after functionalization are summarized in **Table 1**. The polymer content in polymer-*g*-MWNT was analyzed by elemental analysis and expressed as % wt/wt. The amount of immobilized polymer on MWNT was found to be comparable in both PEI-*g*-MWNT and PAA-*g*-MWNT ($\approx 5\%$) and slightly higher in PEI/PAA-*g*-MWNT ($\approx 9\%$) (Table 1). The PEI content in PEI-*g*-MWNT was analyzed by another method using NMR spectroscopy and found to be 5.9% wt/wt which agreed with results obtained by elemental analysis (Supporting Information, Figure S1).

Table 1. Properties of MWNT and polymer-*g*-MWNT.

MWNT type ^{a,b}	Length ^c	% Polymer ^d	% Polymer ^e
Pristine MWNT	$\approx 2 \mu\text{m}$	–	–
MWNT-COOH	$\approx 0.5 \mu\text{m}$	–	–
PEI- <i>g</i> -MWNT	$\approx 0.5 \mu\text{m}$	4.9%	–
PAA- <i>g</i> -MWNT	$\approx 0.5 \mu\text{m}$	4.8%	5.9%
PEI/PAA- <i>g</i> -MWNT	$\approx 0.5 \mu\text{m}$	7.5–10%	–

a) Diameters for all MWNT were between 20 and 40 nm as determined by TEM and SEM. b) Carbon purity for starting pristine MWNT material was more than 99% as stated by the manufacturer and determined by TGA and EDX. c) Determined by TEM and SEM. d) Determined by elemental analysis. e) Determined by NMR spectroscopy.

Raman spectroscopy was used to evaluate the surface chemistry of the MWNT following polymer functionalization. Raman scattering spectra from pristine MWNT and polymer-*g*-MWNT (Supporting Information, Figure S2) are showing the typical resonant peaks for MWNT that possess overall structural integrity. The G-band at $\approx 1600 \text{ cm}^{-1}$ is a more complex spectral feature that is related to tangential mode vibrations. Structural defects show on the D-band, attributed to disorder or to sp³ carbons in the hexagonal framework of the nanotube backbone. D-band intensity at $\approx 1340 \text{ cm}^{-1}$ increased after the conjugation to PEI or PAA, considered an indication that chemical grafting rather than the physical adsorption of the polymer took place. HRTEM (Supporting Information, Figure S1) also showed that the polymer layers wrapped evenly around the nanotubes in all cases and the thicknesses of the polymer layers were found to be of a few nanometers. Notably, the thickness of the polymer layers grown on different sections of the nanotube and on different nanotubes was similar due to higher degree of functionalization. The physical and morphological characteristics of the pristine, oxidized, and polymer-*g*-MWNT were studied using TEM, SEM (data not shown), and light microscopy (Table 1 and **Figure 1**). The average length of polymer-*g*-MWNT conjugates was found to be about 0.5 μm with a diameter in the range of 20–40 nm. TEM and SEM characterization showed that polymer coupling did not modify the dimensions (length and diameter) of the nanotubes. However, polymer grafting improved the aqueous dispersibility and debundling of MWNT as shown by light microscopy and TEM images (Figure 1). Nevertheless, PAA-*g*-MWNT exhibited lower aqueous dispersibility compared to other polymer-*g*-MWNT. Microscopy analysis showed that the pristine and oxidized MWNT (Figure 1) appeared mostly as nanotube aggregates, whereas the PEI-*g*-MWNT, PAA-*g*-MWNT, and PEI/PAA-*g*-MWNT were significantly debundled and generally appeared as individualized nanotube dispersions.

3.1. Complexation of Polymer-*g*-MWNT with pDNA

Agarose gel electrophoresis demonstrated the ability of polymer-*g*-MWNT to bind pDNA, since only free pDNA was able to migrate in the gel (**Figure 2**). Upon complexation of pDNA with the nanotubes the fluorescent signal (due to EtBr intercalation with the nucleic acid bases) was either quenched or retained in the wells depending on the degree of pDNA condensation. In the case of PEI-*g*-MWNT, complete complexation with pDNA was observed at 3:1 PEI-*g*-MWNT:pDNA mass ratio (1.17 N/P ratio) (Figure 2a). In the case of PAA-*g*-MWNT (Figure 2b), complexation with pDNA was significantly compromised even at 120:1 PAA-*g*-MWNT:pDNA mass ratio (34.8 N/P ratio) (data not shown). As elemental analysis had previously indicated PAA grafting to MWNT, we considered that the overall positive charge of the PAA-*g*-MWNT construct available to complex pDNA must be reduced compared to free PAA alone (Figure 2e). Grafting a mixture of PEI and PAA polymers on the MWNT improved pDNA complexation compared to PAA-*g*-MWNT,

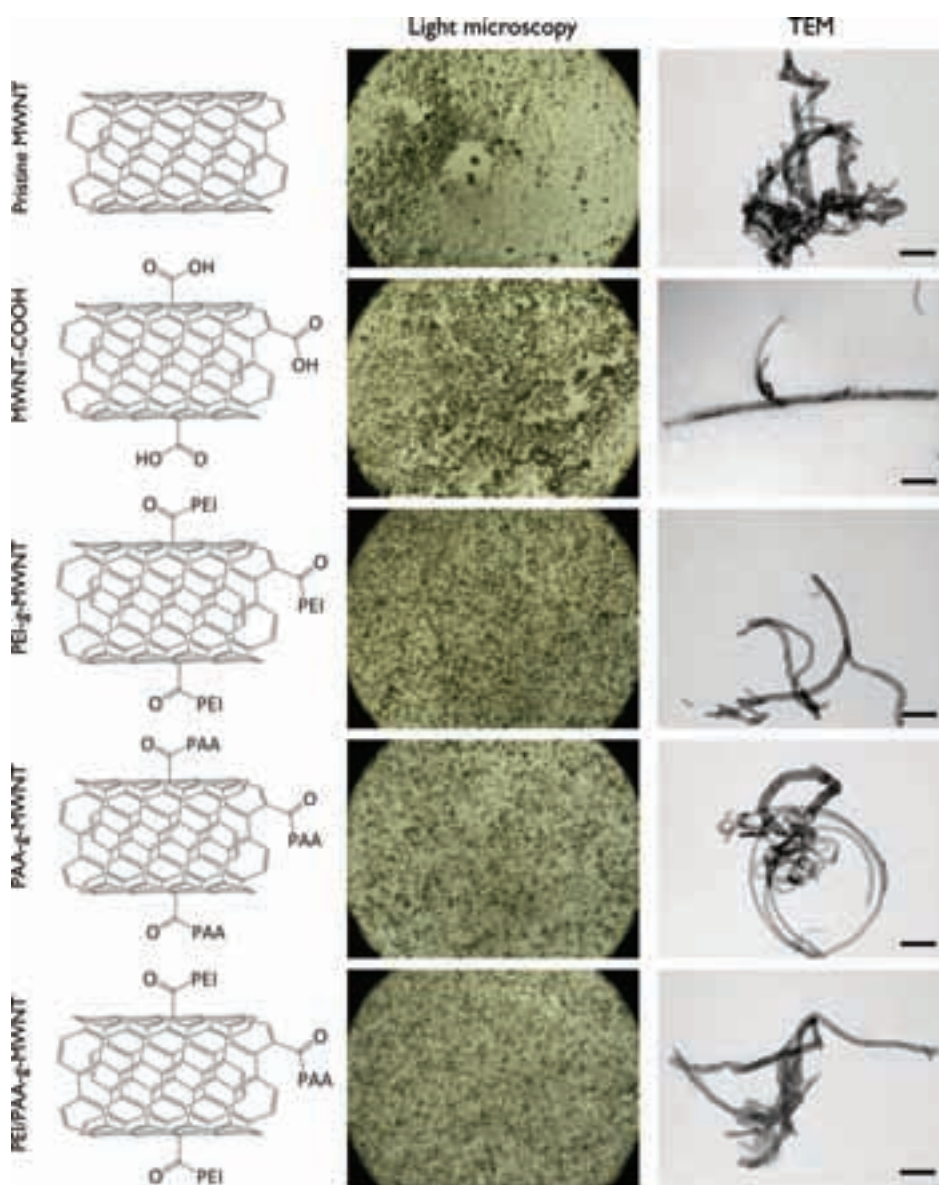


Figure 1. Features of polymer-*g*-MWNTs. Chemical structure of MWNTs, light microscopy images (250x total magnification), and electron microscopy images (TEM) of MWNTs and polymer-*g*-MWNTs dispersed in 5% dextrose at 250 $\mu\text{g mL}^{-1}$ final concentration. Scale bar in TEM images is 100 nm.

with complete restriction of pDNA gel migration occurring at 10:1 PEI/PAA-*g*-MWNT:pDNA mass ratio (Figure 2c). PEI polymer complexed pDNA at 0.1:1 PEI:pDNA mass ratio (0.8 N/P ratio), while PAA polymer complexed pDNA at 0.2:1 PAA:pDNA mass ratio (1.2 N/P ratio). A mixture of PEI and PAA (1:1 mass ratio) complexed pDNA at 0.3:1 mass ratio (Figure 2dE).

3.2. In vitro Gene Expression using Polymer-*g*-MWNT

The ability of both polymer and polymer-*g*-MWNT to induce gene expression was evaluated following incubation with human lung carcinoma (A549) cells (Figure 3). Vectors were complexed with pDNA and incubated with

A549 cells for 24 h, when β -galactosidase expression was assessed. PEI-*g*-MWNT was shown to enhance gene expression in comparison to naked pDNA at all mass ratios tested, most efficiently at the 30:1 PEI-*g*-MWNT:pDNA mass ratio. Contrary to that, PAA-*g*-MWNT did not improve gene expression over naked pDNA at any mass ratios tested. The PEI/PAA-*g*-MWNT construct exhibited the ability to enhance gene expression in comparison to both naked pDNA and individual polymer-*g*-MWNT, with highest levels of gene expression obtained at the lowest (10:1 and 20:1) mass ratios. PEI alone was also included in this study as a positive control under the same conditions used for the polymer-*g*-MWNT transfections. Highest gene expression was obtained at a PEI:pDNA mass ratio of 1:1 (equivalent to 8 N/P ratio) (Supporting Information,

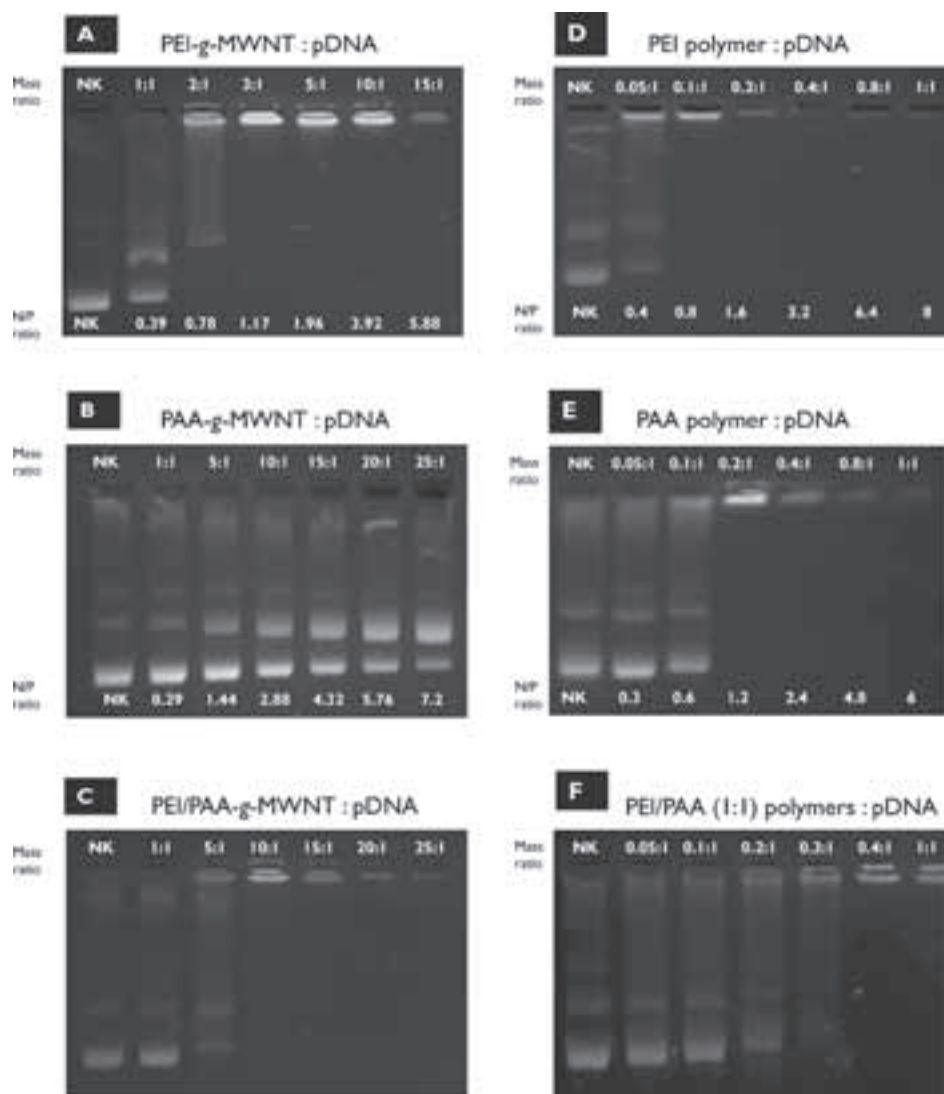


Figure 2. Agarose gel electrophoresis assay of pDNA complexed with A) PEI-g-MWNT, B) PAA-g-MWNT, C) PEI/PAA-g-MWNT, D) PEI polymer, E) PAA polymer, and F) PEI:PAA mixture (1:1). Naked pDNA was used as a reference in all panels. pDNA ($0.5 \mu\text{g}$) was complexed at various mass (or charge) ratios.

Figure S3a). PAA polymer alone was not successful in achieving gene transfer and expression in A549 cells under these experimental conditions (Supporting Information, Figure S3a). Mixtures of free PEI/PAA polymers were also studied for gene transfection that led to enhanced gene expression when compared to individual PEI or PAA polymers, especially when mixed at equal mass ratios (Supporting Information, Figure S3b). On the other hand, mixing the individual PEI-g-MWNT with PAA-g-MWNT did not improve the transfection efficiency over the PEI-g-MWNT alone either at 15:1 or 20:1 mass ratio (Supporting Information, Figure S3c).

3.3. In vitro Toxicity

Cytotoxicity is a critical factor for successful gene delivery. In this study, toxicity of the polymer-g-MWNT compared to free polymers in A549 cells was assessed

by a modiPced LDH assay.^[24,25] After 24 h incubation period, cell viability indicated that both free PEI and PAA polymers were causing significant cytotoxicity at concentrations higher than 5 and $40 \mu\text{g mL}^{-1}$, respectively (Figure 3b). The PEI-g-MWNT and PAA-g-MWNT constructs did not affect cell viability up to $80 \mu\text{g mL}^{-1}$ (maximum tested), while the PEI/PAA-g-MWNT was shown to lead to significant cytotoxicity at $40 \mu\text{g mL}^{-1}$ and above.

3.4. Intracellular Trafficking of pDNA Complexes in A549 Cells

In order to assess whether gene expression efficiency was directly associated with the degree in pDNA cell internalization after complexation with various polymers or polymer-g-MWNT vectors, we performed trafficking experiments using confocal laser scanning microscopy (CLSM). Fluorescently labeled pDNA (fluorescein; green) was complexed with the nanotubes and subsequently incubated with A549 cells.

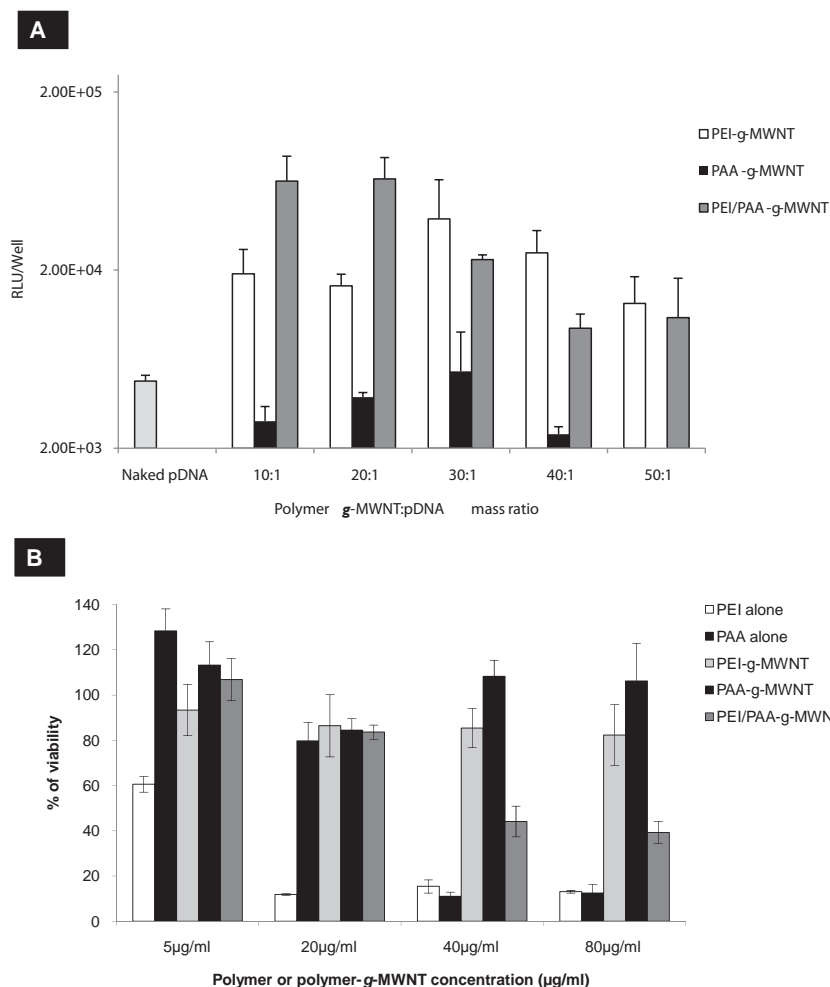


Figure 3. A) Gene transfection efficiency in human lung carcinoma (A549) cells after transfection with polymer-*g*-MWNT: pDNA complexes at various mass ratios. pDNA encoding for β -galactosidase enzyme was complexed with the vectors and incubated with the cells at final pDNA concentration of $2 \mu\text{g mL}^{-1}$ ($1 \mu\text{g}$ per well) and gene expression was assessed 24 h post-transfection and expressed as average RLU per well \pm SD ($n = 3$). B) Modified LDH cytotoxicity assay performed after 24 h incubation of A549 cells with either the free polymer or polymer-*g*-MWNT.

The complexes were removed after 4 h and the cells were fixed and imaged by CLSM at 4 h and 24 h time points. Cells were also stained with Cy3-labeled anti-EEA1 antibody for visualization of the early endosomes (red) and with TO-PRO3 for counterstaining the nucleus (blue). The pattern of polyplex pDNA internalization was different from that of pDNA complexed with the polymer-*g*-MWNT (**Figure 4**). The polyplexes led to localization of the pDNA within the endosomes (evidenced by the colocalized green and red signals) especially at the 4 h time point, with subsequent pDNA release from the endosome after 2 h except for the case of PAA alone (where pDNA endosomal release was minimal). The results reported here for the free PEI and PAA polymers suggest the endosomal pathway as the main route for internalization of pDNA as has been reported in the literature.^[26,28]

In the case of polymer-*g*-MWNT:pDNA vectors, most of the internalized complexes were not colocalized within endosomes and larger, more aggregated complexes were observed

to accumulate in the cytoplasm (Figure 4). No significant differences among the different polymer-*g*-MWNT:pDNA complexes studied in terms of colocalization with endosomal markers were observed. Moreover, the kinetics of the pDNA internalisation seemed to occur at a slower rate compared to the polyplexes as evidenced by the lower green fluorescence intensity signals at 4 h. Interestingly, PEI/PAA polyplexes appeared more aggregated than the PEI/PAA-*g*-MWNT:pDNA complexes (Figure 4) after 24 h, where these aggregates appeared to be outside the cell membrane.

These trafficking studies suggested that the polymer-*g*-MWNT constructs may facilitate a route of cellular internalization for the complexed pDNA alternative to that followed by the free polymer:pDNA complexes.

4. Discussion

We have previously reported carbon nanotube-mediated delivery of pDNA using ammonium *f*-CNT, which illustrated the ability of chemically functionalized cationic CNT to bind pDNA efficiently and enhance gene transfer.^[2,3] From these results, we concluded that the nanotube surface charge density and consequent formation of the complex are critical parameters for the interaction of CNT with pDNA.^[2,3] These original studies were followed by Liu et al.^[15] that described the use of PEI-*g*-CNT for efficient gene transfer and expression.

The present study presents further attempts to functionalize CNT with different cationic polymers for the purpose of improving gene expression in vitro. MWNT grafted with PEI, PAA, or a mixture of both polymers, were well dispersed in aqueous media (Figure 1). Elemental analysis indicated the grafting of PAA polymer in PAA-*g*-MWNT, which was similar in content to that of PEI in the PEI-*g*-MWNT construct, Raman microscopy confirmed the polymer chemical conjugation. pDNA complexation with free polymer or polymer-*g*-MWNT was confirmed by agarose gel electrophoresis (Figure 2). A difference in binding affinity between these materials and pDNA was observed with binding affinities in the following order: PEI (0.8 N/P ratio) > PEI-*g*-MWNT (1.17 N/P ratio) > PAA (1.2 N/P ratio) > PEI/PAA > PEI/PAA-*g*-MWNT > PAA-*g*-MWNT (30 N/P ratio). Due to their high cationic charge, PEI and PAA have been previously shown to bind pDNA efficiently^[20,21,29] at low N/P ratios.^[1,30] Conjugation of PEI and PAA polymers to MWNT resulted in a different pDNA binding profile. PAA-*g*-MWNT did not bind pDNA

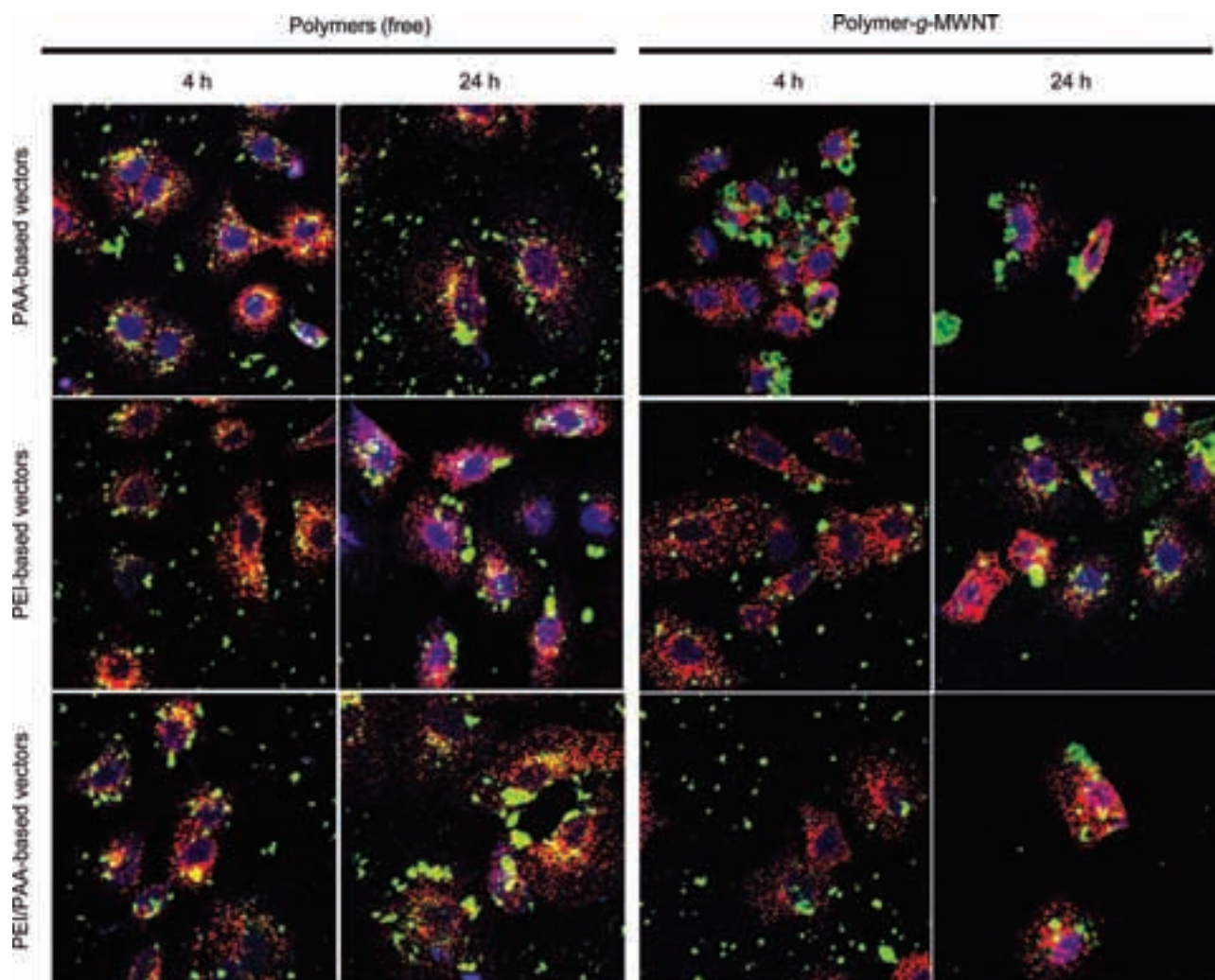


Figure 4. Intracellular trafficking of polymer:pDNA or polymer-g-MWNT:pDNA complexes after 4 h and 24 h incubation with A549 cells. Fluorescently labeled pDNA was used to track pDNA uptake, (green), endosomes were stained with Cy3-labeled anti-EEA1 antibodies (red), and nuclei were counterstained with TO-PRO 3 (blue).

efficiently even up to very high mass ratios (120:1), while PEI-g-MWNT complexation occurred at low (10:1) mass ratio. In addition, agarose gel electrophoresis showed that both polymers mixed or in the free form were able to bind pDNA efficiently. We concluded that immobilization of PAA onto the MWNT greatly reduced its binding efficiency to pDNA. We also observed that both PEI-g-MWNT and PEI/PAA-g-MWNT complexed the pDNA however, the latter being significantly less effective. Although structural analysis to explain the variation in pDNA complexation needs further investigation, we propose that branched PEI covalently immobilized on the MWNT surface have a high content of primary, secondary, and tertiary amines that can still serve as effective plasmid condensation sites leading to immobilization of pDNA.^[15] In comparison, the linear structure of PAA may lead to neutralisation of the primary PAA amines on interaction with the carboxyl groups at the oxidized MWNT backbone. Such charge neutralisation of the free primary amines of PAA can explain the greatly reduced pDNA complexation observed (Figure 2).

Assembly of PAA polymer molecules on the surface of carboxylated MWNTs has been previously reported by others^[31] in a similar fashion as described, even though for a non-biological application.

The in vitro gene expression data in A549 cells correlated with the results obtained from the pDNA binding studies. PAA and PAA-g-MWNT were consistently found to be inefficient gene transfer vectors under the experimental conditions used (Figure 3 and the Supporting Information, Figure S3a) and efficient gene transfer and expression was obtained in the case of PEI, PEI-g-MWNT, and PEI/PAA-g-MWNT. PEI is known for its ability to bind pDNA and promote the intracellular release from the endosome via the proposed proton sponge effect as first suggested by Behr et al.^[4,15,20,29] Cationic polymers can have a buffering capacity between pH 5.0 and 7.2 and have shown to induce osmotic swelling and consequently endosome rupture.^[32] Thus, the nucleic acid endosomal content can be released in the cytoplasm,^[1,32] thus our studies with PAA:pDNA complexes suggested inability of free PAA polymer to escape the endosomal compartment with the

consequent poor levels of gene expression (Supporting Information, Figure S3a). PAA does not have buffering capacity^[1,4] due to the presence of non-titratable primary amino groups and the lack of titratable secondary and tertiary amino functions, which are thought responsible for the buffering capacity of PEI.^[1,21] Moreover, as described by Suh et al.,^[33] the protonation of PAA may occur to a lesser degree compared with PEI, in particular at basic pH.^[33]

The PEI/PAA-g-MWNT achieved greater gene expression in comparison to PEI-g-MWNT especially at lower mass ratios. Such improvement in gene expression could be obtained due to the properties of the polymer mixture, where PAA reduces the compact nature of the complex by lowering the overall positive charge of PEI/PAA-g-MWNT and therefore facilitates pDNA release from the complex after internalization.^[2] However, free PEI/PAA polymer mixture (1:1 mass ratio) and PEI polymer alone showed higher levels of gene expression compared to those achieved with polymer-g-MWNT.

Although Liu et al.^[15] reported similar transfection efficiency for PEI-g-MWNT and PEI polymer, according to the TGA analysis, the percentage of PEI conjugated to the MWNT surface was around 8.2% compared to only 5% in this study. Moreover, their study was performed in different cell lines (COS7, HepG2, and 293 cell lines), using a different gene report (pCMV-Luc), and for 48 h at 2 µg pDNA dose. The novelty we report for the hybrid polymer-g-MWNT construct here is the ability to achieve better efficiency at lower polymer-g-MWNT concentration by including PAA polymer into PEI-g-MWNT construct.

Several studies have highlighted safety concerns regarding the use of cationic polymers in gene therapy.^[1,4,15,34] The polycationic character of PAA or PEI has been pointed out as a cause for concern regarding cell viability.^[1] Here, we report that the mixed PAA/PEI-g-MWNT was more toxic than PEI-g-MWNT or PAA-g-MWNT at equivalent concentrations. More experiments are needed to establish the mechanism of toxicity of the PAA/PEI-g-MWNT conjugate, however, it is important to note that cell viability was compromised at concentrations higher than 40 µg mL⁻¹ (Figure 3b). An improvement in gene transfer and expression was achieved at concentrations lower than 40 µg mL⁻¹. These results are in line with those of Liu et al.^[15] which showed a toxicity threshold of PEI-g-MWNT at concentrations even below 100 µg mL⁻¹ in three different cell lines up to.^[15] Shen et al.^[34] reported toxic effect of PEI-g-MWNT in FRO cells and KB cells lines at concentrations of 10 µg mL⁻¹ and 50 µg mL⁻¹, respectively. Over all, this emphasises the importance of multiple factors affecting cell viability such as the polymer type and its molecular weight, the cell line used, and the incubation time points while performing cytotoxicity studies.

More importantly, in this study we elucidated that polymer-g-MWNT:pDNA complexes may facilitate a different internalization pathway from conventional polyplexes. The reason for such a difference in intracellular localization of polymer-g-MWNT:pDNA and the lack of colocalization of the vectors within endosomes suggests either energy-independent translocation or phagocytosis (receptor-mediated endocytosis but not clathrin-dependent endocytosis) as possible mechanisms of uptake, in

which the size affect the trafficking kinetics. More mechanistic studies are warranted in order to establish the mechanism by which these polymer-g-MWNT:pDNA complexes enter cells and release their genetic payload intracellularly.

Overall, we attempted to enhance the gene expression capabilities of chemically functionalized MWNT by synthesis of different water-dispersible polymer-g-MWNT. Three constructs: i) PEI-g-MWNT, ii) PAA-g-MWNT, and iii) PEI/PAA-g-MWNT were comparatively studied. All polymer-g-MWNT were able to complex pDNA with different binding efficiencies. PEI/PAA-g-MWNT was found to be the most optimum polymer-g-MWNT for gene transfer due to its capacity to enhance gene expression at minimum nanotube:pDNA mass ratios which was found non-toxic. Mechanistically, pDNA was delivered by the polymer-g-MWNT constructs via a different pathway compared to those used by polyplexes. Such studies further highlight the potential of *f*-CNT as a versatile tool for efficient gene transfer.

Supporting Information

Supporting Information is available from the Wiley Online Library or from the author.

Acknowledgements

We are grateful to our colleague Mr. Samir Hammoud from ZWE-Analytic, Max Plank Institute for Metal Research, Stuttgart, Germany for the performance of elemental analysis. Financial support from the European Union FP6 NINIVE (NMP4-CT-2006-033378) is acknowledged. Figure 3a was replaced on October 18, 2010 because the previous version was corrupted.

- [1] A. Pathak, A. Aggarwal, R. K. Kurupati, S. Patnaik, A. Swami, Y. Singh, P. Kumar, S. P. Vyas, K. C. Gupta, *Pharm. Res.* **2007**, *24*, 1427.
- [2] D. Pantarotto, R. Singh, D. McCarthy, M. Erhardt, J. P. Briand, M. Prato, K. Kostarelos, A. Bianco, *Angew. Chem. Int. Ed.* **2004**, *43*, 5242.
- [3] R. Singh, D. Pantarotto, D. McCarthy, O. Chaloin, J. Hoebeke, C. D. Partidos, J. P. Briand, M. Prato, A. Bianco, K. Kostarelos, *J. Am. Chem. Soc.* **2005**, *127*, 4388.
- [4] S. Nimesh, A. Goyal, V. Pawar, S. Jayaraman, P. Kumar, R. Chandra, Y. Singh, K. C. Gupta, *J. Controlled Release* **2006**, *110*, 457.
- [5] S. H. Huh, H. J. Do, H. Y. Lim, D. K. Kim, S. J. Choi, H. Song, N. H. Kim, J. K. Park, W. K. Chang, H. M. Chung, J. H. Kim, *Biologicals* **2007**, *35*, 165.
- [6] I. S. Kim, S. K. Lee, Y. M. Park, Y. B. Lee, S. C. Shin, K. C. Lee, I. J. Oh, *Int. J. Pharm.* **2005**, *298*, 255.
- [7] M. C. P. de Lima, S. Neves, A. Filipe, N. Duzgunes, S. Simoes, *Curr. Med. Chem.* **2003**, *10*, 1221.
- [8] C. Klumpp, K. Kostarelos, M. Prato, A. Bianco, *Biochim. Biophys. Acta* **2006**, *1758*, 404.
- [9] L. Lacerda, A. Bianco, M. Prato, K. Kostarelos, *J. Med. Chem.* **2008**, *18*, 17.

- [10] N. W. S. Kam, Z. A. Liu, H. J. Dai, *Angew. Chem. Int. Ed.* **2006**, *45*, 577.
- [11] L. Lacerda, S. Raffa, M. Prato, A. Bianco, K. Kostarelos, *Nano Today* **2007**, *2*, 38.
- [12] L. Z. Gao, L. Nie, T. H. Wang, Y. J. Qin, Z. X. Guo, D. L. Yang, X. Y. Yan, *ChemBioChem* **2006**, *7*, 239.
- [13] D. Cai, J. M. Mataraza, Z. H. Qin, Z. P. Huang, J. Y. Huang, T. C. Chiles, D. Carnahan, K. Kempa, Z. F. Ren, *Nat. Methods* **2005**, *2*, 449.
- [14] N. W. S. Kam, Z. Liu, H. J. Dai, *J. Am. Chem. Soc.* **2005**, *127*, 12492.
- [15] Y. Liu, D. C. Wu, W. D. Zhang, X. Jiang, C. B. He, T. S. Chung, S. H. Goh, K. W. Leong, *Angew. Chem. Int. Ed.* **2005**, *44*, 4782.
- [16] J. Rojas-Chapana, J. Troszczyńska, I. Firkowska, C. Morsczech, M. Giersig, *Lab Chip* **2005**, *5*, 536.
- [17] Z. H. Zhang, X. Y. Yang, Y. Zhang, B. Zeng, Z. J. Wang, T. H. Zhu, R. B. S. Roden, Y. S. Chen, R. C. Yang, *Clin. Cancer Res.* **2006**, *12*, 4933.
- [18] M. Ahmed, X. Z. Jiang, Z. C. Deng, R. Narain, *Bioconjugate Chem.* **2009**, *20*, 2017.
- [19] A. Kumar, P. K. Jena, S. Behera, R. F. Lockey, S. Mohapatra, *J. Biomed. Nanotechnol.* **2005**, *1*, 392.
- [20] U. Lungwitz, M. Breunig, T. Blunk, A. Gopferich, *Eur. J. Pharm. Biopharm.* **2005**, *60*, 247.
- [21] O. Boussif, T. Delair, *Bioconjugate Chem.* **1999**, *10*, 877.
- [22] S. Nimesh, R. Kumar, R. Chandra, *Int. J. Pharm.* **2006**, *320*, 143.
- [23] V. Raffa, G. Ciofani, S. Nitodas, T. Karachalios, D. D'Alessandro, M. Masini, A. Cuschieri, *Carbon* **2008**, *46*, 1600.
- [24] H. Ali-Boucetta, K. Al-Jamal, K. Kostarelos, *Methods Mol. Biol.* **2010**, in press.
- [25] C. Samorì, H. Ali-Boucetta, R. Sainz, C. Guo, F. Maria Toma, C. Fabbro, T. da Ros, M. Prato, K. Kostarelos, A. Bianco, *Chem. Commun.* **2010**, *46*, 1494.
- [26] X. Z. Han, Q. Y. Fang, F. Yao, X. N. Wang, J. F. Wang, S. L. Yang, B. Shen, *Cytotechnology* **2009**, *60*, 63.
- [27] S. Brunner, E. Furtbauer, T. Sauer, M. Kurs, E. Wagner, *Mol. Ther.* **2002**, *5*, 80.
- [28] C. L. Duvall, A. J. Convertine, D. S. Benoit, A. S. Hoffman, P. S. Stayton, *Mol. Pharm.* **2010**.
- [29] W. T. Godbey, K. K. Wu, A. G. Mikos, *Proc. Natl. Acad. Sci. USA* **1999**, *96*, 5177.
- [30] Y. Lee, M. Y. Cho, H. Mo, K. Nam, H. Koo, G. W. Jin, J. S. Park, *Bull. Korean Chem. Soc.* **2008**, *29*, 666.
- [31] H. J. Park, J. Kim, J. Y. Chang, P. Theato, *Langmuir* **2008**, *24*, 10467.
- [32] J. P. Behr, *Chimia* **1997**, *51*, 34.
- [33] J. Suh, H. J. Paik, B. K. Hwang, *Bioorg. Chem.* **1994**, *22*, 318.
- [34] M. W. Shen, S. H. Wang, X. Y. Shi, X. S. Chen, Q. G. Huang, E. J. Petersen, R. A. Pinto, J. R. Baker, W. J. Weber, *J. Phys. Chem. C* **2009**, *113*, 3150.

Received: May 21, 2010
Published online: September 13, 2010